NEOPLASIA
www.neoplasia.com

Volume 19 Number 10 October 2017 pp. 805–816 805

Molecular Imaging of Colorectal Tumors by Targeting Colon Cancer Secreted Protein-2 (CCSP-2)

Jaeil Kim[*,1], Eun-ju Do[†,1], Helen Moinova[‡], Sang Mun Bae[†], Ja Young Kang[†], Seung-Mo Hong[§], Stephen P. Fink[‡], Jinmyoung Joo[†,¶], Young-Ah Suh[#], Se Jin Jang[§], Sung Wook Hwang[**], Sang Hyoung Park[**], Dong-Hoon Yang[**], Byong Duk Ye[**], Jeong-Sik Byeon[**], Jaewon Choe[*,**], Suk-Kyun Yang[**], Sanford D. Markowitz[‡,††], Sang-Yeob Kim[†,¶] and Seung-Jae Myung[†,**]

*Health Screening & Promotion Center, Asan Medical Center, Seoul, Republic of Korea; [†]Asan Institute for Life Sciences, Asan Medical Center, Seoul, Republic of Korea; [‡]Department of Medicine, Case Western Reserve University, Cleveland, OH, USA; [§]Department of Pathology, Asan Medical Center, University of Ulsan College of Medicine, Seoul, Republic of Korea; [¶]Department of Medicine, University of Ulsan College of Medicine, Seoul, Republic of Korea; [#]Institute for Innovative Cancer Research, Asan Institute for Life Sciences, Asan Medical Center, Seoul, Republic of Korea; [**]Department of Gastroenterology, Asan Medical Center, University of Ulsan College of Medicine, Seoul, Republic of Korea; [††]University Hospitals Seidman Cancer Center, Case Western Reserve University, Cleveland, OH, USA

Abstract

A versatile biomarker for detecting colonic adenoma and colon cancer has yet to be developed. Colon cancer secreted protein-2 (CCSP-2) is a protein specifically expressed and secreted in colon adenomas and cancers. We developed a fluorescent imaging method based on CCSP-2 targeting for a more sensitive and specific detection of colorectal tumors. CCSP-2 expression was evaluated in human colon adenoma and colorectal specimens. Anti–CCSP-2 antibody was labeled with a near-infrared fluorescent dye, FPR-675, and molecular imaging of surgical human colorectal tumors was performed. Immunohistochemistry identified CCSP-2 expression in 87.0% of colorectal cancer specimens and 89.5% of colon adenoma specimens. Fluorescence imaging of surgical human colon specimens after spraying treatment with the probe permitted a clear distinction of cancer from paired normal colon tissue (target-to-background ratio, 4.09 $\pm$ 0.42; $P < .001$). CCSP-2 targeting imaging was also evaluated in patient-derived colon cancer xenograft mouse and liver metastasis murine models. CCSP-2–positive colon cancer xenografts and liver metastases were visualized by near-infrared fluorescence imaging after intravenous injection of the probe, which showed significantly higher fluorescence. Our results show that CCSP-2 is a promising marker for colorectal tumor detection in clinical settings and that a CCSP-2–targeting molecular imaging strategy might improve the diagnosis of colorectal tumors in metastatic or recurrent cancers and aid in early colonoscopic detection of premalignant lesions.

Neoplasia (2017) 19, 805–816

Address all correspondence to: Seung-Jae Myung, Department of Gastroenterology and Convergence Medicine, University of Ulsan College of Medicine, Asan Medical Center, 88 Olympic-Ro 43-gil, Songpa-gu, Seoul 05505, Republic of Korea or Sang-Yeob Kim, Department of Convergence Medicine, University of Ulsan College of Medicine & Asan Institute for Life Sciences, Asan Medical Center, Olympic-Ro 43-gil, Songpa-gu, Seoul 05505, Korea, or Sanford D. Markowitz, Department of Medicine, Case Western Reserve University, and University Hospitals Seidman Cancer Center, Cleveland, Ohio, USA.

E-mails: sxm10@cwru.edu; sykim3yk@amc.seoul.kr; sjmyung@amc.seoul.kr

[1] J. K. and E.-J. D. contributed equally to this work.

Received 21 April 2017; Revised 17 July 2017; Accepted 24 July 2017

1476-5586
http://dx.doi.org/10.1016/j.neo.2017.07.003

Introduction

Colorectal cancer (CRC) is the second leading cause of cancer-related death in Western societies, with a high lifetime incidence [1]. A significant proportion of CRC cases and resulting mortalities can be prevented by colonoscopic detection and removal of adenomas or early-stage neoplasms [2–5]. Consequently, in an average-risk general population, participation in screening colonoscopy decreases the risk of CRC development by 48% to 67% and the risk of death from CRC by 65% [6].

Although conventional white-light colonoscopy has high sensitivity, it is prone to missing flat or depressed lesions that are potentially invasive, thereby resulting in progression to large advanced lesions by the time of diagnosis [7–9]. Furthermore, detection of early cancers by conventional colonoscopy is difficult in patients with long-term ulcerative colitis or Crohn's disease [10,11] because colitis-related CRCs are usually multifocal and flat and may be more difficult to distinguish from chronic colitis-associated background inflammation [12–14]. Accordingly, a more sensitive imaging-based tumor lesion detection technique is needed.

Currently emerging optical molecular imaging techniques based on molecular cell signatures for targeted gastrointestinal imaging have yielded promising results [15–23]. Optical probes with near-infrared fluorescence (NIRF) allow improved photon penetration through tissues and minimizes the effects of tissue autofluorescence [24–27]. Joshi et al. [18] and Kelly et al. [20] have utilized a NIRF-labeled disease-specific peptide probe for early CRC detection, and Mitsunaga et al. [28] validated the utility of a topically applied enzymatically activatable probe (gGlu-HMRG) for fluorescence colonoscopic detection of colitis-related CRC *in vivo* in an AOM/DSS mouse model [28]. Previously, our group utilized NIRF-emitting quantum dots conjugated to matrix metalloproteinase (MMP) 9, MMP 14, and carcinoembryonic antigen (CEA) antibodies to specifically target CRC with a simultaneous "spray and wash" technique [29]. These studies suggested a future clinical application of this novel technology; however, specific imaging of CRC was incomplete due to the lack of a specific probe targeting a specific biomarker. Also, no biomarker has been reported to be expressed in both premalignant and malignant colon cancer.

Colon cancer secreted protein-2 (CCSP-2) is a stably circulating protein also known as von Willebrand factor A domain-containing protein 2, which has two epidermal growth factor domains and three von Willebrand factor type A domains. Expression of CCSP-2 is generally absent in the normal colon but is dramatically upregulated in colon adenomas and CRCs with a mean of 78-fold increase in primary CRC compared to matched normal mucosa [30]. Here, we aimed to perform molecular imaging of human colorectal tumor with a NIRF probe conjugated to an antibody against CCSP-2 in *ex vivo* and *in vivo* human colon tumors and evaluated the ability of this technique for detecting colorectal tumors.

Materials and Methods

Immunohistochemistry (IHC)

Human colon tissue specimens were fixed for 24 hours in 10% neutral buffered formalin and embedded in paraffin. CCSP-2 immunostaining was performed using a BenchMark XT automatic immunostaining device (Ventana Medical Systems, Tucson, AZ) and OptiView DAB IHC Detection Kit (Ventana Medical Systems) according to the manufacturer's instructions. Four-micrometer–thick sections were obtained with a microtome, transferred onto silanized charged slides, allowed to dry for 10 minutes at room temperature, and incubated for 20 minutes at 65°C. Sections were subjected to heat-induced epitope retrieval with Cell Conditioning 1 buffer for 64 minutes and incubated with anti–CCSP-2 antibody (1:100) in the autoimmunostainer for 32 minutes. Antigen-antibody reactions were visualized with a Ventana OptiView DAB IHC Detection Kit (OptiView HQ Linker 8 minutes, OptiView HRP Multimer 8 minutes, OptiView H_2O_2/DAB 8 minutes, OptiView Copper 4 minutes). Staining intensity was graded as absent (0), weak positive (1+), or strong positive (2+).

CCSP-2–Targeted NIRF and Control Probes

NIRF probe was produced for CCSP-2 targeting in colorectal tumors. Briefly, the NIR dye FPR-675 (peak absorption, 675 nm; peak emission, 698 nm) was purchased from BioActs (Incheon, Korea). Anti–CCSP-2 antibody was labeled with the fluorescent dye (CCSP-2–targeted probe) according to the manufacturer's protocol. Briefly, the antibody was dissolved in 1 ml of 0.1 M sodium bicarbonate buffer (pH 9.5), and FPR-675 NHS ester dye was dissolved in DMSO at 10 mg/ml. While stirring, 50 to 100 μl of reactive dye solution was slowly added to the antibody solution, followed by 1-hour incubation at room temperature in the dark. Purification was accomplished using a PD-10 desalting column (GE Healthcare, Waukesha, WI) after diluting the peptide in phosphate-buffered saline (PBS). Product fractions were pooled and assessed with a NanoDrop 2000 Spectrophotometer (Thermo Fisher Scientific, Wilmington, MA) to determine the coupling degree, which was 2.5 to 3.0. As a control, mouse mAb IgG1 isotype control (Cell Signaling Technology, Beverly, MA) was labeled with the same fluorescent dye as the anti–CCSP-2 antibody (control probe).

Cancer Cell Lines and Culture Conditions

Human CRC cell lines SW620 and HCT116 were obtained from American Type Culture Collection (Manassas, VA). Cells were maintained in RPMI-1640 and DMEM (Gibco Laboratories, Grand Island, NY) supplemented with 10% FBS (Hyclone, Logan, UT) and 1% antibiotic-antimycotic (Gibco Laboratories). All cell lines were grown at 37°C in 5% CO_2.

Construction of CCSP-2–Overexpressing Cells

HCT116 cells were seeded onto 35-mm dishes (1×10^6 cells/dish) and transfected with 2 μg of CCSP-2-V5/His-tagged plasmid in 100 μl of Lipofectamine 2000 Reagent (Invitrogen, Carlsbad, CA) according to the manufacturer's protocol. CCSP-2–overexpressing cells were selected with 1 mg/ml geneticin (G418; Gibco Laboratories) 2 days after transfection. Individual stable clones were isolated and assayed for CCSP-2 protein production.

Immunoblotting

CCSP-2–overexpressing cells (HCT116/CCSP-2) and corresponding controls were seeded onto 35-mm dishes (1×10^6 cells/dish). After cells were allowed to secrete CCSP-2 into medium for 24 hours, the 1 ml of cell culture medium was collected. The culture medium was centrifuged for 5 minutes at 1500*g*, and the supernatant was transferred the new tube. Equal amounts of protein (30 μg) were separated by 10% SDS polyacrylamide gel electrophoresis and electroblotted to PVDF membranes. Blotted membranes were blocked with 5% dry milk in Tris-buffered saline–Tween 20 at

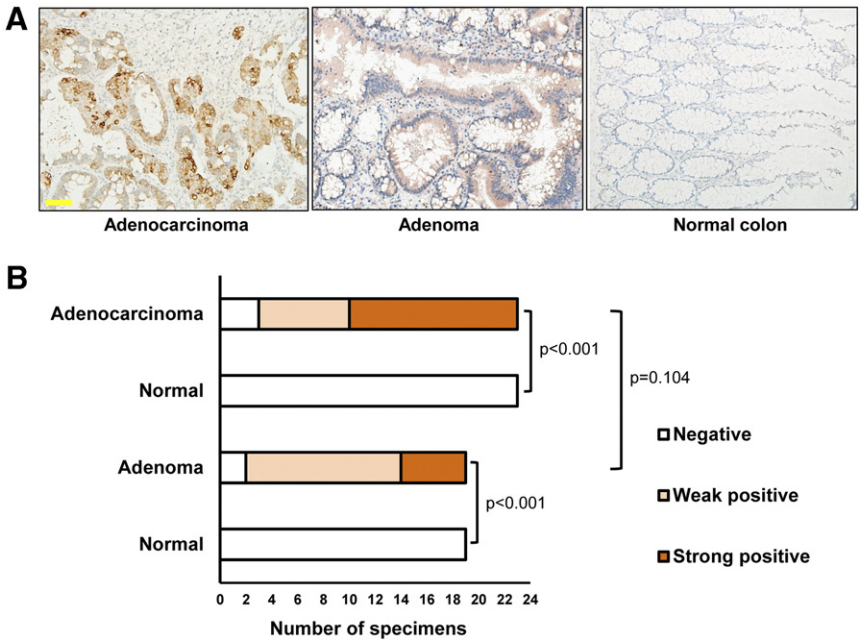

Figure 1. (A) Representative immunohistochemical images of a human CRC and colon adenoma. Original magnification, 200×. Scale bar: 50 μm. (B) Significantly stronger CCSP-2 expression was observed in human CRCs and adenomas compared with paired normal colon tissues (each $P < .001$, marginal homogeneity test).

room temperature for 1 hour and incubated with diluted anti–CCSP-2 antibody (1:500) as primary antibody. Horseradish peroxidase–conjugated anti-mouse IgG (1:7000; Cell Signaling Technology) was used as a secondary antibody. An enhanced chemiluminescence detection kit (Amersham Biosciences, Little Chalfont, UK) was used to detect specific labeled proteins. Membranes were developed using an enhanced chemiluminescence system (Amersham Pharmacia Biotech, Inc., Piscataway, NJ).

In Vitro CCSP-2–Targeted Probe Binding Study

The ability of CCSP-2–targeted probe for detecting CCSP-2 overexpression was tested *in vitro*. CCSP-2–overexpressing cells (HCT116/CCSP-2) and control cells were seeded in 6-well plates (15,000 cells/well) and incubated in culture medium for 1 day. For binding studies, cells were washed once with PBS and fixed with 4% paraformaldehyde (Wako, Osaka, Japan) at room temperature for 10 minutes. After two PBS washes, cells were blocked in Protein Block Serum-Free (Dako, Carpinteria, CA) and were permeabilized with 0.1% Triton X-100 in PBS for 15 minutes. After two further PBS washes, CCSP-2–targeted probe (3.2 μg/ml) was added to each well. After a 10-minute incubation period at room temperature, cells were washed twice with PBS and counterstained with the nuclear stain 4,6-diamidino-2-phenylindole (DAPI; Invitrogen). Cell suspensions were evaluated on a Zeiss LSM780 confocal microscope (Carl Zeiss, Jena, Germany).

Ex Vivo Molecular Imaging of Human Colorectal Tumors

Frozen human colon specimens (8-10 mm) were obtained through the Asan Bio Resource Center. Fifteen CRC specimens and 6 colon adenoma specimens from 21 patients were halved to compare CCSP-2–targeted and control probe staining. Autofluorescence images of the tumor specimen and paired normal colon specimen were obtained prior to probe incubation. Tumor specimens were thawed to room temperature and incubated in 48-well plates with CCSP-2–targeted probe (30 μg/ml) or control probe for 1 hour. Paired normal colon tissue specimens were also incubated with CCSP-2–targeted probe. After incubation, tissue specimens were washed three times with PBS to clear unbound antibody and subjected to fluorescence imaging (Optix MX3 system; ART Advanced Research Technologies Inc., Montreal, Canada). *Ex vivo* molecular imaging was correlated with histopathology and immunochemistry.

Ex Vivo Molecular Imaging of Fresh Surgical Human CRC Specimen

Human colon samples (14-20 mm) were surgically excised from three patients. Each fresh, unfixed CRC specimen with adjacent normal colon specimen was delivered immediately following removal. CRC specimen was halved to compare CCSP-2–targeted probe and free NIRF dye (FPR-675) staining. To avoid a possible false-positive result from probe infiltration of the cut surfaces, the cut surface of the tissue specimen was covered with low–melting point agarose gel. CRC specimens were incubated with CCSP-2–targeted probe (30 μg/ml) or free NIRF dye for 30 minutes. Adjacent normal colon tissue specimens were also incubated with CCSP-2–targeted probe. After incubation, tissue specimens were washed three times with PBS, and molecular (NIRF) images were acquired. To visualize *ex vivo* CCSP-2–targeted probe binding during incubation, cryosections were subjected to confocal microscopy without CCSP-2 restaining. Sections were stained with FITC mouse anti-E-cadherin (BD Transduction Laboratories, San Diego, CA) for 2 hours at 1:100 dilution at room temperature.

Xenograft Mouse Models of CRC

Patient-derived CRC xenograft (PDX) mouse models were established using tissues surgically removed from a patient. These tissues were removed and cultured to establish primary cancer cell lines. The cultured cells were implanted in 6- to 8-week-old

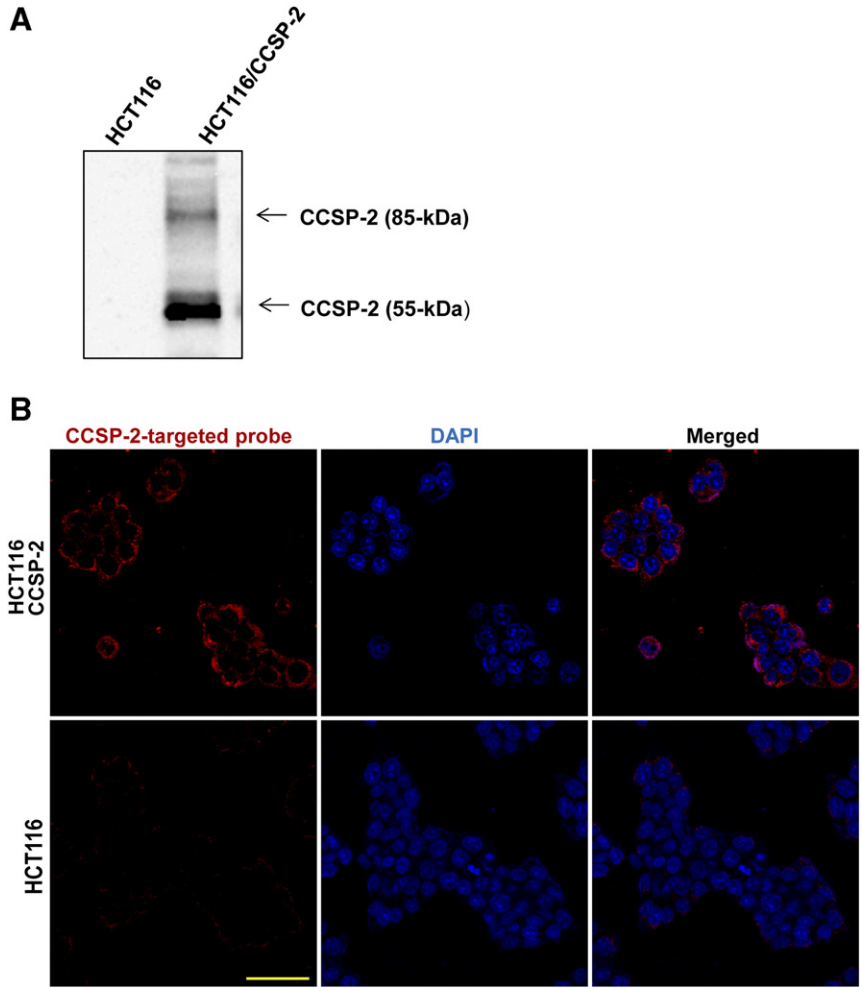

Figure 2. *In vitro* CCSP-2–targeted probe binding study. (A) Western blot showing overexpression of CCSP-2 in HCT116 cells transfected with a CCSP-2–encoding plasmid. Arrowheads denote the positions of the full-length 85-kDa CCSP-2 protein and 55-kDa CCSP-2–derived peptide detected in the lysates of CCSP-2–transfected cells. (B) CCSP-2–overexpressing cells (HCT116/CCSP-2) and corresponding control cells (HCT116) were incubated with CCSP-2–targeted probe. *In vitro* confocal microscopy of the cell cultures confirmed binding of the CCSP-2–targeted probe (red) to CCSP-2–overexpressing cells, whereas control cells showed no CCSP-2 staining. Nuclei were counterstained with DAPI (blue). Original magnification, 400×. Scale bar: 50 μm.

immunodeficient NOD/SCID mice (Charles River Laboratories Japan, Inc., Yokohama, Japan). Once reaching an approximate size of 1 cm^3, tumors were removed and transferred to male BALB/c nude mice (Orient Bio Inc., Seongnam, South Korea). In addition, 10^7 SW620 cells were suspended in 120 µl of PBS and subcutaneously injected into the thighs of BALB/c nude mice. Once PDX and SW620 xenograft tumors reached 5 to 7 mm in diameter, the mice were used for *in vivo* molecular imaging studies.

In Vivo Molecular Imaging of CRC Xenograft Mouse Models

CCSP-2–targeted (n = 6) or control (n = 3) probe was intravenously injected into the tail vein of PDX mice (1.2 µg/g body weight); CCSP-2–targeted probe was also intravenously injected into SW620 xenograft mice (n = 3). Molecular (NIRF) images were acquired at 3, 6, 12, and 24 hours and 2 and 3 days after injection. To evaluate probe biodistribution, molecular images of isolated organs (tumor, normal colon, kidney, liver, and lung) were acquired immediately after the mice were sacrificed 3 or 4 days after injection. To visualize *in vivo* bound CCSP-2–targeted probe, xenograft tumor and normal colon cryosections were subjected to confocal microscopy without CCSP-2 restaining.

Mouse Models of CRC Liver Metastasis

HCT116-CCSP-2–overexpressing cells were seeded onto 24-well plates (50,000 cells/well) and received 10 µl of lentiviral particles via 200 µl of RediFectTM (PerkinElmer Inc., Norwalk, CT) according to the manufacturer's protocol. HCT116-CCSP-2-RediFectTM cells were selected with 2 µg/ml puromycin (Sigma-Aldrich) after 2 days of virus infection. To obtain a mouse model of CRC liver metastasis, 3×10^6 HCT116-CCSP-2-RediFectTM cells were suspended in 100 µl of PBS and injected into the spleen of BALB/c nude mice. For operative procedures, mice were anesthetized with tribromoethanol (Avertin, Sigma-Aldrich). A 1-cm laparotomy was performed, and the spleen was exteriorized. The spleen was divided into two; one part was left in the mouse, and the other part was used as a route for the injection. The prepared cells were injected into the exposed hemispleen, and the injected hemispleen was eliminated. The abdomen was closed with absorbable 5-0 Vicryl sutures and the

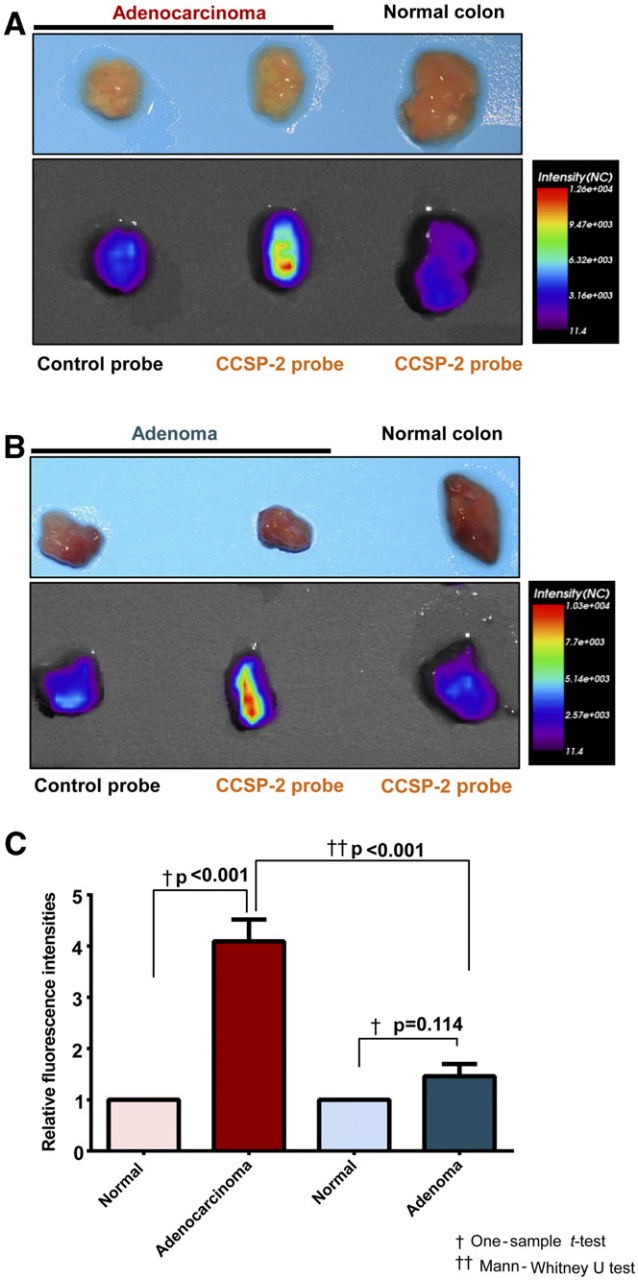

Figure 3. *Ex vivo* molecular imaging of a human colorectal tumor. (A) Representative *ex vivo* molecular imaging of a human CRC specimen. The CRC specimen showed significantly elevated signal intensity relative to the paired normal colon specimen. (B) *Ex vivo* molecular imaging of a human colon adenoma specimen. (C) Relative fluorescence intensities of colorectal tumors versus paired normal colon tissues (tumor-to-background fluorescence ratios). Bars indicate SEM.

skin with skin clips. The animals were sacrificed 3 to 4 weeks after tumor cell injection.

In Vivo Molecular Imaging of CRC Liver Metastasis

To confirm the presence of liver metastases, bioluminescence images were obtained using the Xenogen IVIS spectrum system (Caliper Life Sciences, Inc., Hopkinton, MA) before probe injection. For bioluminescence imaging, mice were intraperitoneally injected with D-Luciferin (Gold Biotechnology, St. Louis, MO) at a dose of 150 μg/g mouse body weight 10 minutes before imaging. Mice were then placed in a chamber with 3% isoflurane and transferred to the IVIS imaging chamber. Images were acquired using a 20-cm field of view and 0.5- to 1.0-minute exposure time. CCSP-2–targeted probe (1.2 μg/g body weight) was intravenously injected into the tail vein of liver metastasis mouse model mice (n = 5) and normal control mice (n = 5). Molecular (NIRF) images were obtained at 1, 2, 3, and 4 days after injection. Molecular images of isolated organs (liver, spleen, kidney, lung, and colon) were acquired immediately after the mice were sacrificed 4 days after injection. Tissues of metastatic liver tumors were homogenized in lysis buffer (50 mM Tris-HCL, pH 7.4, 100 mM NaCl, 10 mM $CaCl_2$, 0.25% Triton X-100, protein inhibitor cocktail). Immunoblotting was performed as above described method. An anti–β-actin antibody (1:10,000; Sigma-Aldrich Co., St. Louis, MO) was used as loading control.

Molecular Imaging Analysis

All molecular imaging procedures except liver metastasis imaging were performed using the Optix MX3 system (ART Advanced Research Technologies Inc.). The excitation wavelength was set at 675 nm for NIRF dye (FPR-675) excitation. NIRF emission was detected and recorded at 695 nm. OptiView software (version 2.02.00; ART Advanced Research Technologies Inc.) was used to quantify light emission in the selected region of interest as total photon counts. Fluorescence intensities were expressed as mean intensities in selected areas. Target-to-background ratios (TBRs) were calculated by dividing the fluorescence intensity of the tumor by that of paired normal colon. Molecular imaging and bioluminescence imaging procedures of liver metastasis were performed using the Xenogen IVIS spectrum system (Caliper Life Sciences, Inc.).

Statistical Analysis

Data are reported as mean ± standard error of the mean (SEM). Marginal homogeneity test and Fisher's exact test were applied for statistical analyses of immunochemical data. Significant differences in the calculated TBRs between colorectal tumor and paired normal colon tissues were evaluated using a one-sample t test. Between-group comparisons of continuous variables were assessed using Mann-Whitney U test. Significance tests were two-tailed, and significance was defined at $P < .05$. Statistical analyses were performed using SAS 9.4 version for Windows (SAS Institute Inc., Cary, NC).

Ethics Approval

All animal experiments and procedures were conducted in compliance with the Principles of Laboratory Animal Care formulated by the Institutional Animal Care and Use Committee of the Asan Institute for Life Sciences, Asan Medical Center. The institutional review board of Asan Medical Center (IRB No. 2013-1070) approved this study. Biospecimens and data used in this study were provided by Asan Bio-Resources Center, Korea Biobank Network [2014_2(71)].

Results

CCSP-2 Upregulated in Human CRC and Adenoma

We evaluated the expression of CCSP-2 in healthy and diseased human tissues by IHC. Most CRC and adenoma specimens were positive for CCSP-2, which showed predominantly cytoplasmic expression (Figure 1*A*). In contrast, all paired normal colon specimens were negative for CCSP-2 (Figure 1, *A* and *B*). Of 23 CRC

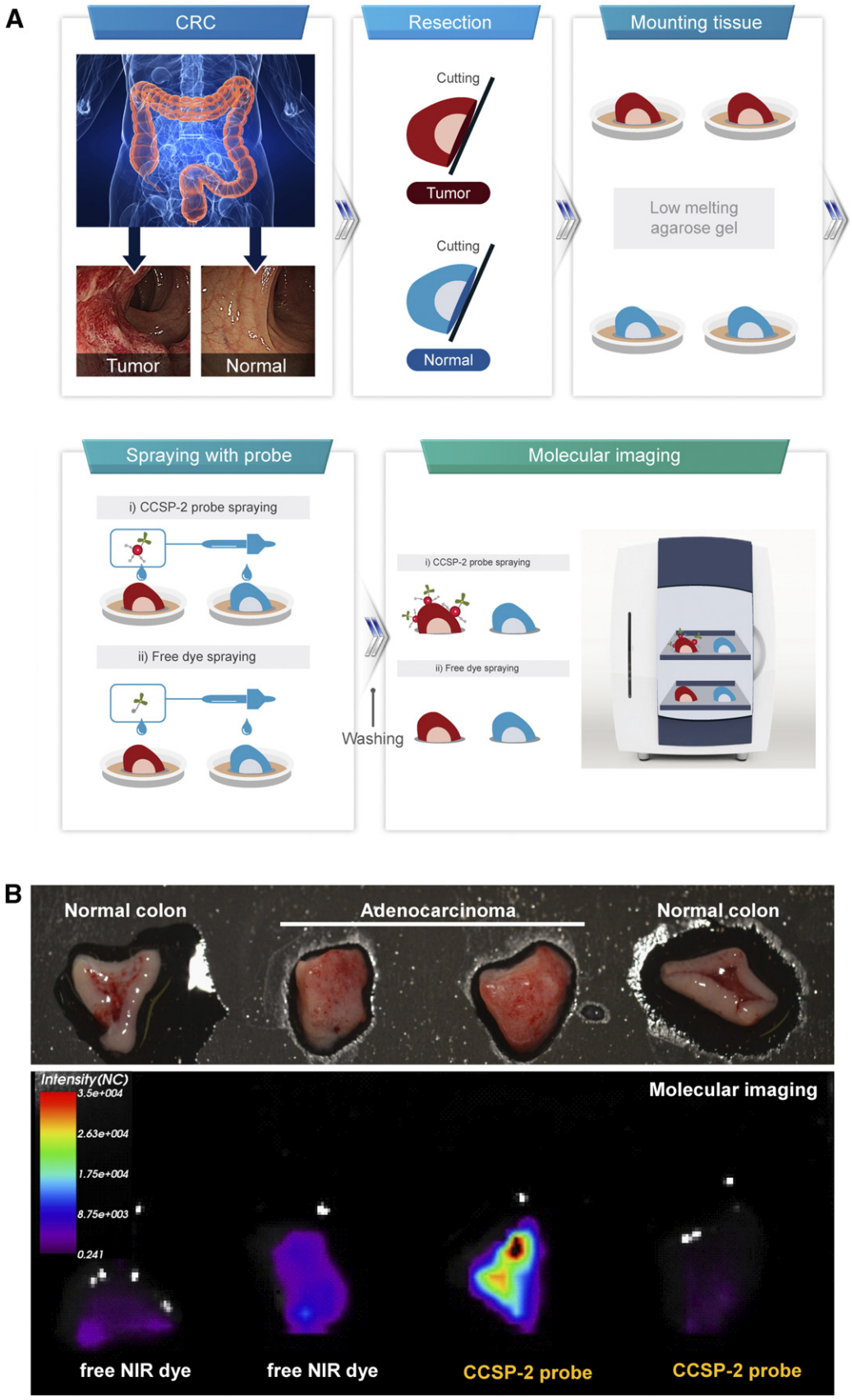

Figure 4. *Ex vivo* molecular imaging of a fresh surgical human CRC specimen. (A) Schematic illustration of the molecular imaging process. (B) Representative molecular image. (C) *Ex vivo* confocal microscopy of cryosections from a fresh surgical human colon tissue specimen. CRC specimens incubated in the CCSP-2–targeted probe showed specific fluorescence signals within tumor tissues. Superimposition of E-cadherin immunofluorescence and DAPI nuclear staining confirms that the CCSP-2–targeted probe signal is located at the cancer cell membranes and cytoplasm. Original magnification, 400×. Scale bar: 50 μm.

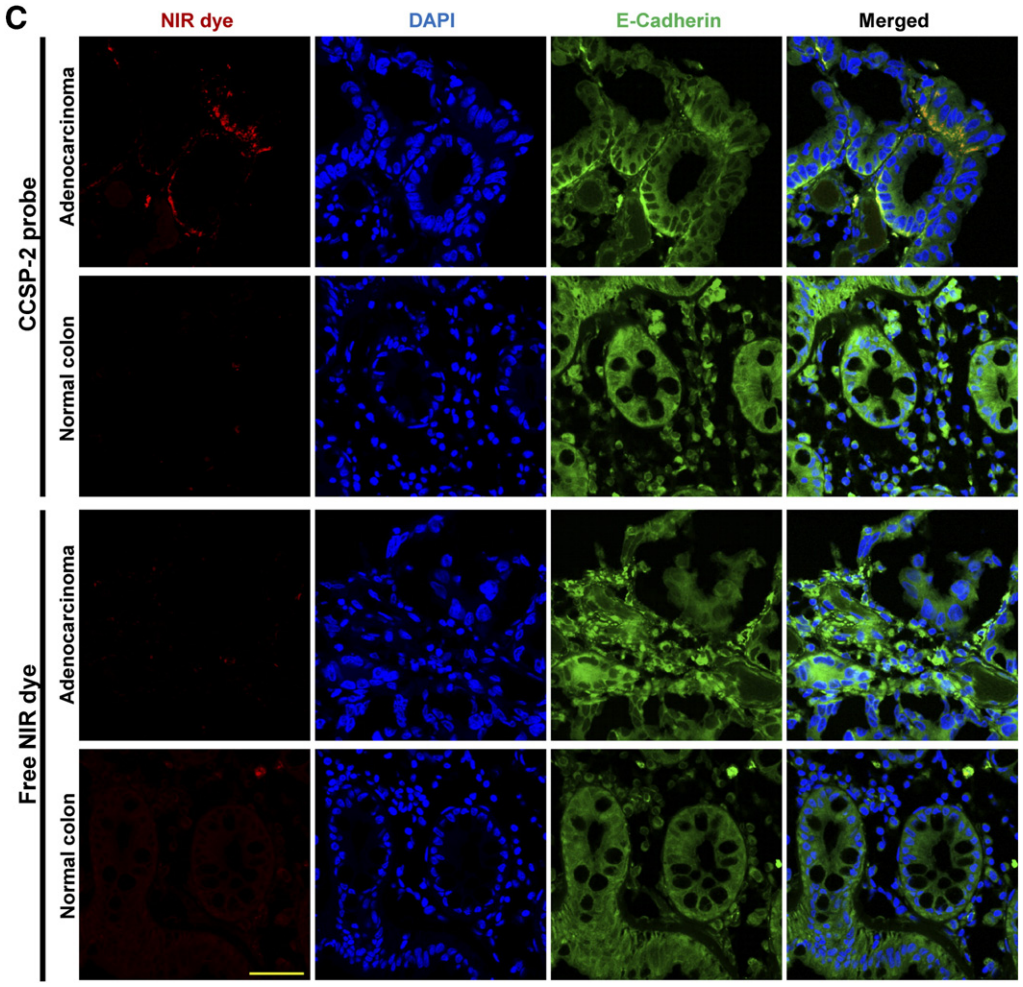

Figure 4. (*continued*).

specimens, 20 (87.0%) showed CCSP-2 overexpression: 13 (56.5%) were strongly positive (2+), and 7 (30.4%) were weakly positive (1+). Of 19 adenoma specimens, 17 (89.5%) showed CCSP-2 overexpression: 5 (26.3%) were strongly positive (2+), and 12 (63.2%) were weakly positive (1+). A tendency toward stronger CCSP-2 expression was observed in CRC samples versus adenomas (P = .104, Fisher's exact test).

In Vitro Characterization of the CCSP-2–Targeted NIRF Probe

HCT116 cells were transfected with a CCSP-2–encoding plasmid, and CCSP-2 expression was measured. Western blot analysis revealed CCSP-2 expression in the plasmid-transfected HCT116 cells (denoted HCT116/CCSP-2), with the expected full-length 85-kDa CCSP-2 protein and a shorter 55-kDa CCSP-2–derived peptide clearly detectable in the lysates of CCSP-2–transfected HCT116 cells but not of control cells (Figure 2*A*). To test the binding ability of the CCSP-2–targeted NIRF probe to CCSP-2–positive and CCSP-2–negative cells, both cell lines were subjected to *in vitro* confocal microscopy after incubation with the CCSP-2–targeted NIRF probe. CCSP-2 antibody binding to CCSP-2–overexpressing HCT116 cells was confirmed, and control cells showed no discernible CCSP-2 staining (Figure 2*B*).

Ex Vivo Molecular Imaging of Human Colorectal Tumor Using the CCSP-2–Targeted NIRF Probe

All CRC specimens (n = 15) showed significantly higher fluorescence intensities than paired normal colon specimens after incubation with a CCSP-2–targeted probe (Figure 3*A*). TBRs were calculated by dividing the fluorescence intensity of the tumor by that of paired normal colon; the mean TBR was 4.09 ± 0.42, with a range of 2.25–7.80 (Figure 3*C*, P < .001, one-sample t test). In contrast, CRC specimens incubated with control probe and paired normal colon specimens incubated with CCSP-2–targeted probe showed similar low signal intensities. IHC against CCSP-2 revealed CCSP-2 expression in 14 CRC specimens from 15 patients and no CCSP-2 expression in paired normal colon specimens.

Only one colon adenoma specimen incubated with the CCSP-2–targeted probe showed high fluorescence intensity relative to the paired normal colon specimen (Figure 3*B*), with a TBR value of 2.5. IHC staining for CCSP-2 indicated weak expression. However, five other adenoma specimens showed similar fluorescence intensities relative to paired normal colon specimens. There were no significant fluorescence intensity differences between adenomas and paired normal colon samples. The mean TBR was 1.45 ± 0.24, with a range of 0.73 to 2.50 (Figure 3*C*, P = .114, one-sample t test). The mean TBR of adenoma was significantly lower than that of CRC (P < .001, Mann-Whitney U test).

Ex Vivo Molecular Imaging of Fresh Surgical Human CRC Tissue Using the CCSP-2–Targeted NIRF Probe

Figure 4*A* shows the overall scheme of molecular imaging experiments involving fresh surgical human CRC specimens. All fresh surgical human CRC specimens (n = 3) showed significantly elevated fluorescence intensities relative to adjacent normal colon specimens

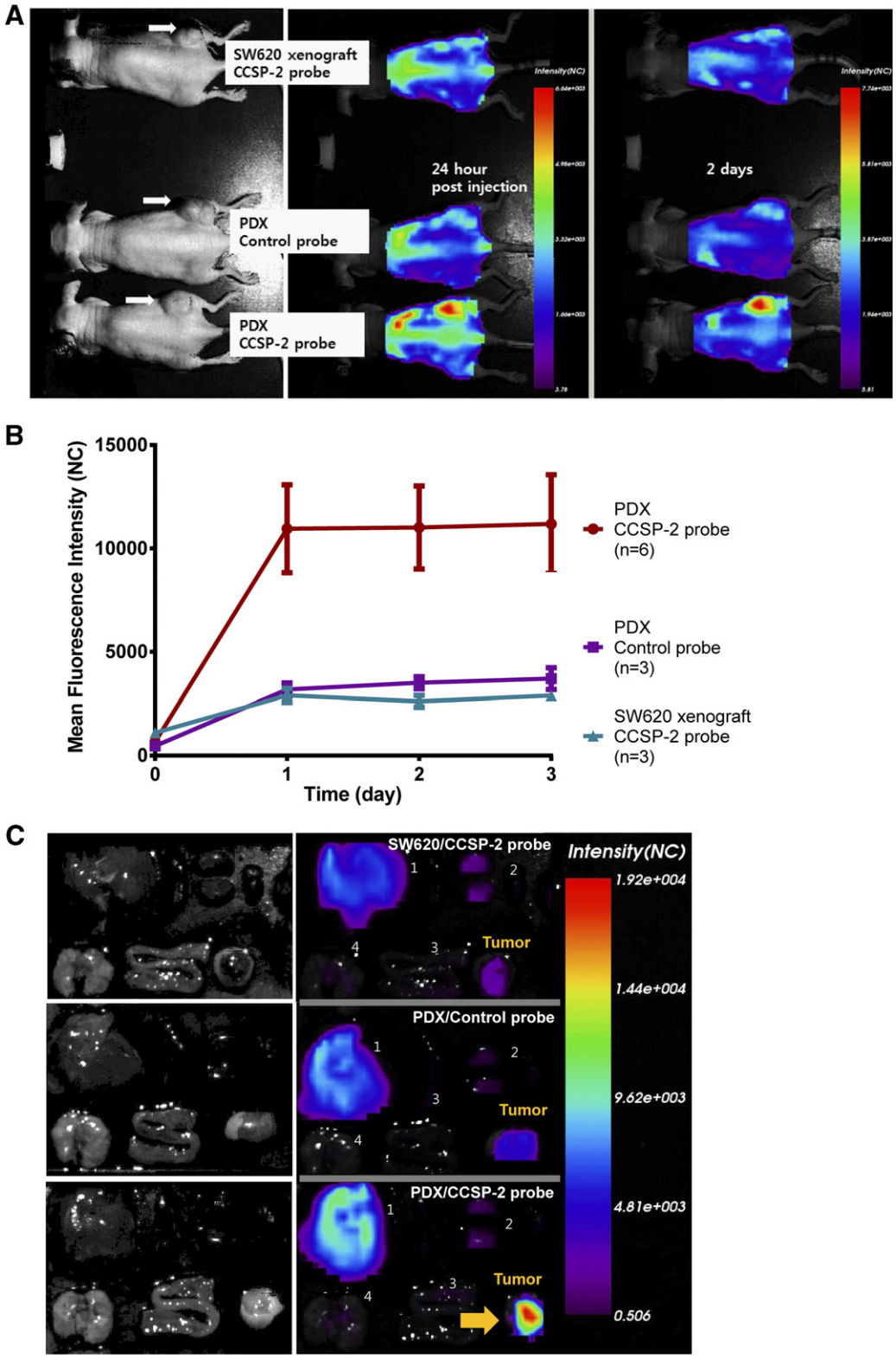

Figure 5. *In vivo* molecular imaging of PDX mouse models. (A) Molecular images of PDX and SW620 xenografts after tail vein injection of a CCSP-2–targeted or control probe. (B) Mean fluorescence in PDX tumors and SW620 xenografts after tail vein injection of a CCSP-2–targeted probe and in PDX tumors after the injection of a control probe at different time intervals. Twenty-four hours after intravenous probe injection, PDX tumors/CCSP-2 probe showed significantly higher fluorescence intensities relative to PDX tumors/control probe ($P = .024$, Mann-Whitney U test) and SW620 xenograft tumors/CCSP-2 probe ($P = .024$, Mann-Whitney U test). Bars indicate SEM. (C) *Ex vivo* molecular images of isolated organs in PDX and SW620 xenograft models were acquired after the mice were sacrificed 3 or 4 days after injection. (1) Liver, (2) kidneys, (3) colon, and (4) lung. PDX tumors injected with a CCSP-2–targeted probe showed the highest probe concentrations. (D) *Ex vivo* confocal microscopy of a PDX tumor injected with CCSP-2–targeted probe confirmed fluorescence after *in vivo* binding of the molecular probe. Nuclei were counterstained with DAPI (blue). Original magnification, 200×. Scale bar: 50 μm.

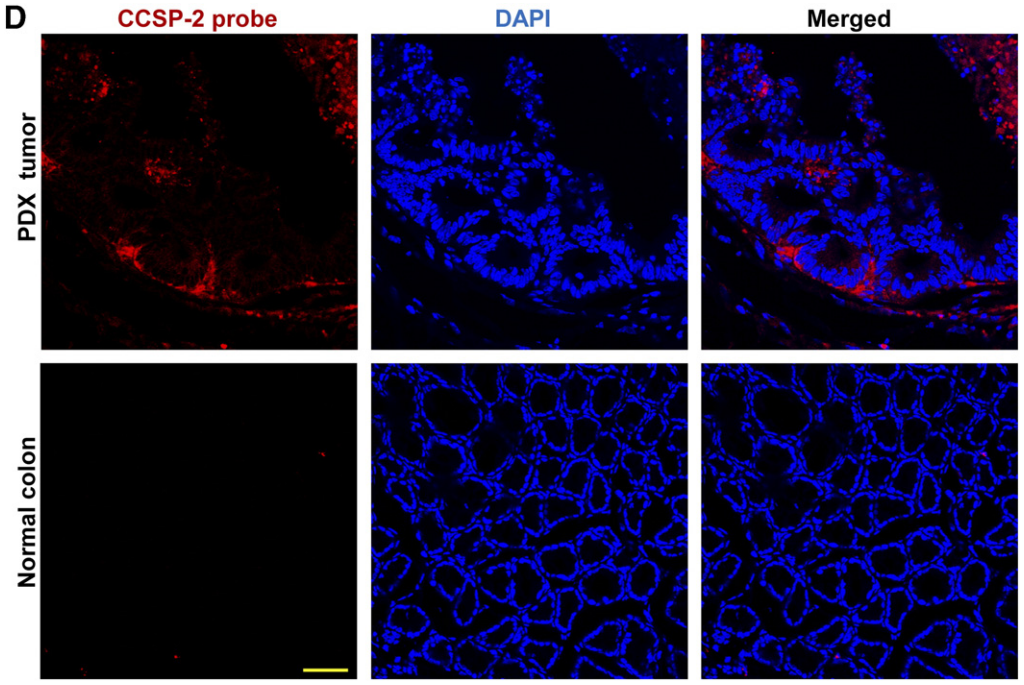

Figure 5. (*continued*).

after incubation with a CCSP-2–targeted probe (Figure 4*B*). The TBRs of samples were 11.74, 6.10, and 15.00. In contrast, CRC treated with free NIRF dye showed relatively low signal intensities. *Ex vivo* confocal microscopy of CRC specimen cryosections incubated in CCSP-2–targeted probe confirmed a cytoplasmic and membranous fluorescence signal within tumor tissues; adjacent normal colon specimens incubated in CCSP-2–targeted probe did not show a specific fluorescence signal. No specific fluorescence signal was observed in CRC and normal colon specimens incubated in untargeted free NIRF dye (Figure 4*C*). IHC revealed CCSP-2 expression in all CRC tissues and no CCSP-2 expression in adjacent normal colon tissues (data not shown).

In Vivo Molecular Imaging of PDX Mouse Models

To evaluate the specificity and effectiveness of the CCSP-2–targeted NIRF probe for *in vivo* application, tumor imaging studies were performed in a subcutaneous PDX model. Twenty-four hours after intravenous injection of CCSP-2–targeted probe, PDX tumors (n = 6) showed high fluorescence intensities, with signal persistence up to 3 days (Figure 5*A*, lower row). Few differences in fluorescence intensity were observed between 24 hours, 2 days, and 3 days after injection (Figure 5*B*). In contrast, CCSP-2–negative SW620 xenograft-bearing mice (n = 3) injected with CCSP-2–targeted-probe and PDX tumor-bearing mice injected with a control probe (n = 3) showed significantly lower fluorescence intensities relative to PDX tumor-bearing mice injected with CCSP-2–targeted probe (Figure 5, *A* and *B*).

Ex vivo fluorescence signals were measured in isolated organs of sacrificed mice to evaluate molecular probe biodistribution. PDX-bearing mice injected with CCSP-2–targeted probe showed the highest probe concentration (Figure 5*C*). The liver, which is the main elimination route of fluorescently labeled antibody elimination, showed a relatively high fluorescence signal. In contrast, CCSP-2–negative SW620 xenografted mice injected with CCSP-2–targed probe and PDX-xenografted mice injected with control probe had low fluorescence intensities (Figure 5*C*). *Ex vivo* confocal microscopy of cryosections of PDX tumors from CCSP-2–targeted probe-injected mice confirmed fluorescence signal within the tumor tissues (Figure 5*D*). IHC confirmed CCSP-2 expression in the parental patient tumor (data not shown).

In Vivo Molecular Imaging of CRC Liver Metastasis Mouse Models

Twenty-four hours after intravenous CCSP-2–targeted probe injection, CCSP-2–positive CRC liver metastases (n = 5) showed significantly higher fluorescence intensities compared with livers without metastases (n = 5) and were clearly visible (Figure 6, *B* and *D*). Using *in vivo* bioluminescent imaging and *ex vivo* molecular imaging of isolated organs from sacrificed mice, we identified liver metastatic lesions (Figure 6, *A* and *C*). Histopathology confirmed the presence of CRC metastases into livers (Figure 6*E*). Western blot analysis confirmed CCSP-2 expression in liver metastatic lesions (Figure 6*F*). This result suggests that the fluorescence from the liver originated from CCCP-2–positive metastatic tumor.

Discussion

In the gastroenterology field, molecular imaging is used to identify and characterize mucosal features *in vivo* based on molecular traits rather than morphological structure [31]. Enhanced molecular target imaging of colorectal tumors would potentially improve the effectiveness of tumor resection as well as enable early detection of resectable CRC recurrence. Molecular probes for tumor imaging usually target tumor-specific biomarkers [32]. The ideal biomarker should be overexpressed in premalignant lesions as well as advanced cancers for the early detection and prevention. Here, we describe a novel colorectal tumor target, CCSP-2, that was overexpressed in nearly 90% of colon adenomas and cancers in our study. By conjugating NIRF dye to anti-CCSP2 antibody, we demonstrate that this technology is effective for identifying human colon cancer. Furthermore, by using murine PDX and metastasis models, we show the potential for the development of a CCSP-2–based imaging method for the detection of metastatic or recurrent cancer outside of the colon.

Molecular probes can be applied topically or systemically. Antibodies are potentially immunogenic and may cause side effects after systemic application; also, accumulation of labeled antibody and

increased nonspecific background staining may occur as well [17]. Clinically, topical application may be more practical and useful during colonoscopy and may be associated with a decreased incidence of immunogenicity and other adverse events [33]. For that purpose, the binding efficacy of CCSP-2–targeted probe to human colon tumor tissues via mucus layer penetration needed to be verified in fresh tissues. We verified the efficacy of our CCSP-2–targeted probe via comparison with *ex vivo* molecular images of surgical human colon tumor specimens stained with a control probe or free NIRF dye solution. In our experiment, to prevent the penetration of the probe via the cut surface of the specimen, we covered the cut surfaces of fresh tissues with agarose gel. Using this procedure, a TBR of >6 was

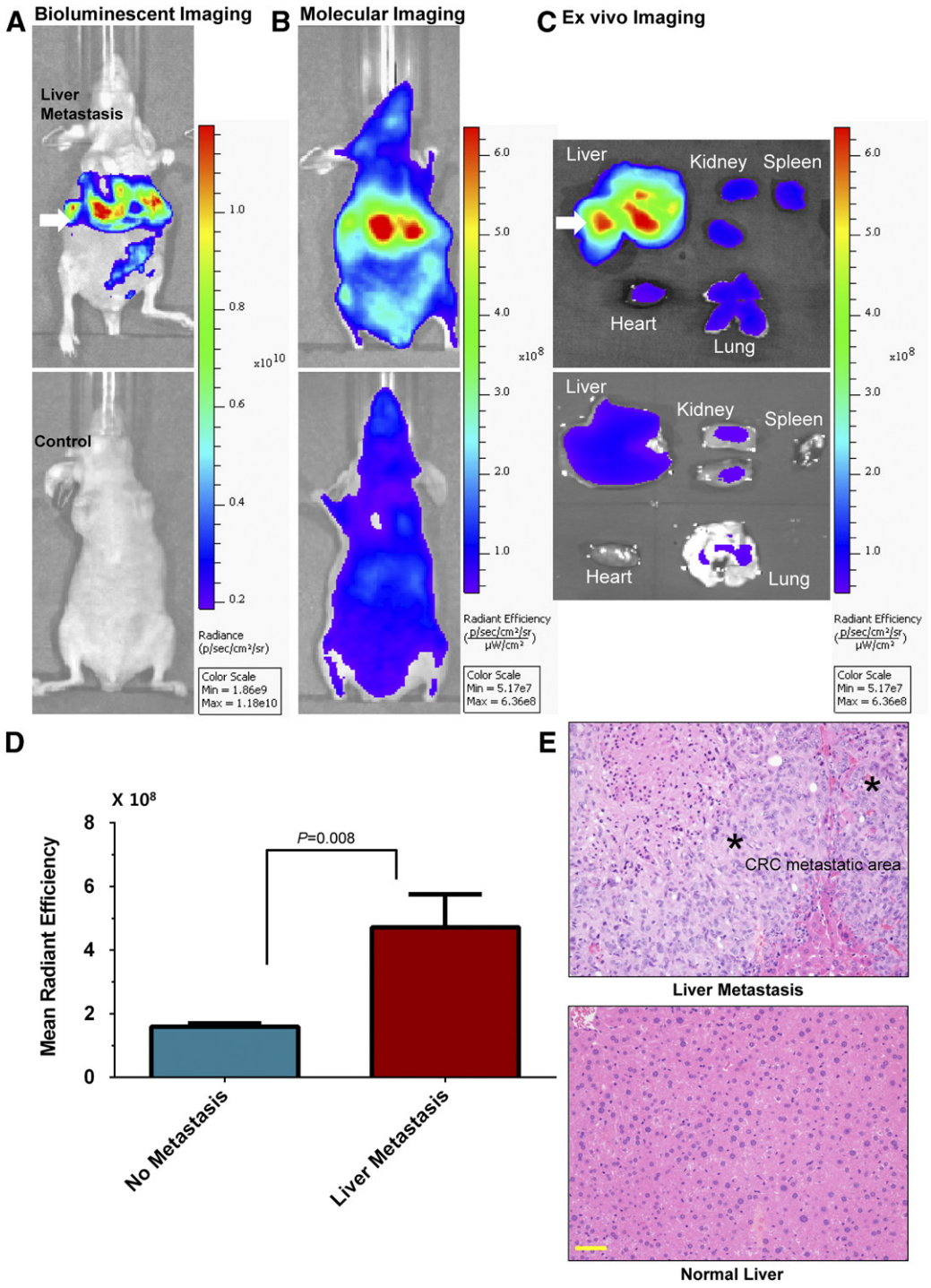

Figure 6. *In vivo* molecular imaging of CRC liver metastasis. (A) Liver metastasis was detected by *in vivo* bioluminescent imaging following intrasplenic injection of HCT116-CCSP-2 bioluminescent cells. (B) Representative molecular image of liver metastasis. (C) *Ex vivo* molecular images of isolated organs. (D) Twenty-four hours after intravenous probe injection, liver metastases showed significantly higher fluorescence intensities relative to normal liver (P = .008, Mann-Whitney U test). Bars indicate SEM. (E) Representative H&E micrographs of the liver metastasis. Original magnification, 200×. Scale bar: 50 μm. (F) Western blot showing overexpression of CCSP-2 in liver metastatic lesions.

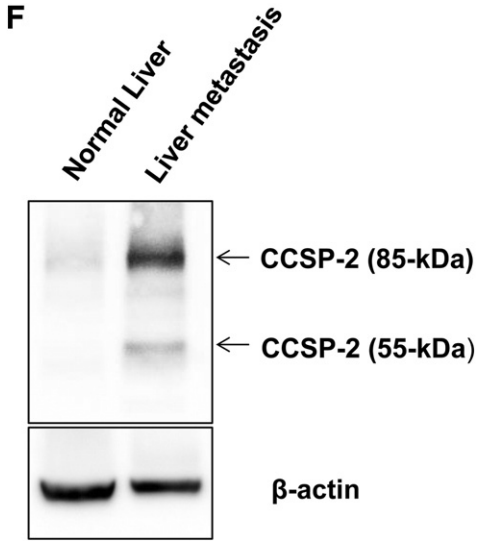

Figure 6. (*continued*).

obtained in comparison with CRC and normal tissues, indicating the specificity and usefulness of this probe for a "spray and wash" molecular imaging method. Interestingly, *ex vivo* confocal microscopy of cryosections from fresh human CRC specimens incubated in CCSP-2–targeted probe revealed a predominantly cytoplasmic, partly membranous fluorescence signal. Further investigation of how CRC cells internalize anti–CCSP-2 monoclonal antibody after CCSP-2 binding is needed.

For the evaluation of molecular probes, the possibility of false-positive result due to the increased vascular permeability of tumors should be considered. Vascular permeability is known to be enhanced in tumors, which permits the entry of macromolecules to the interstitium [34]. Leaky tumor vasculature is responsible for the well-known limitation of fluorescently labeled antibody imaging, namely, nonspecific uptake due to enhanced permeability and retention [25,35]. We accounted for this limitation and verified the efficacy of our target-specific molecular probe by comparing *in vivo* molecular images of both xenograft mouse models obtained with a control probe and control (CCSP-2–negative) xenograft mouse models obtained with a CCSP-2–targeted probe.

In our experiments using PDX and CRC liver metastasis mouse models, we demonstrated that CCSP-2–targeted probe can identify extracolonic CCSP-2–positive colon tumors. These findings suggest that CCSP-2–targeting molecular imaging may also be able to detect metastatic disease. For the treatment of colon cancer, intensive follow-up and detection of early metastatic or recurrent disease may improve patient survival [36,37]. However, there are some patients whose relapse is not diagnosed even with conventional imaging and CEA testing until the cancer has progressed to a late stage. More sensitive and specific techniques such as CCSP-2 imaging or serum CCSP-2 detection will save more patients by detecting lesions during the early stage of the disease.

Both our developed probe and its specific target CCSP-2 are promising options for clinical imaging. However, this probe should be further modified for clinical use. A short incubation time (i.e., a few minutes) is mandatory for topical endoscopic use; however, the optimum incubation times in our study were 1 hour (frozen human colon specimen) or 30 minutes (fresh human colon specimen). Some adenoma specimens did not show high fluorescence intensity relative to paired normal colon specimens, possibly due to relatively weaker CCSP-2 expression compared with CRC. Another explanation might be slow diffusion rate of the high–molecular-weight fluorescently labeled antibodies across epithelial borders and slow delivery to target structures [19]. Importantly, CCSP-2 expression was confirmed using immunohistochemistry in about 90% of colon adenoma specimens. Accordingly, these shortcomings of our CCSP-2–targeted probe could be overcome by using peptide-based probes with better tumor penetration. Low–molecular affinity peptides offer good affinity, rapid binding kinetics, and deep penetration into the altered mucosa [17,20,38,39]. Development of CCSP-2–targeted radionuclide probes would be a viable option for systemic administration and detection of metastatic or recurrent cancer.

Our results demonstrate the benefits of CCSP-2–specific NIRF imaging, which are attributable to the ability of this technique to discriminate CRC from normal tissues. Fluorescence endoscopy involving NIRF imaging with a CCSP-2–targeted probe in combination with conventional endoscopy, namely, a multispectral endoscopic system, might be useful for the detection of remnant neoplastic tissue after endoscopic resection of CRC and early colorectal tumors in patients with long-term ulcerative colitis or Crohn's disease. In addition, CCSP-2–targeted imaging is expected to evolve and become more sensitive and specific for the detection of metastatic and recurrent cancer.

Conclusion

CCSP-2, a novel protein that is distinctly expressed in adenomas and CRC, is a promising marker for colorectal tumor detection. Our study demonstrates the feasibility of molecular imaging with a CCSP-2–targeted probe in surgical human colon cancer specimens and in PDX and liver metastasis mouse models for CRC. In the future, novel CCSP-2–targeted probe-based molecular imaging techniques might be useful for the detection of early colorectal tumors and metastatic or recurrent diseases.

Conflicts of Interests

There are no potential conflicts of interest to disclose.

Acknowledgements

We thank Dr. Joon Seo Lim from the Scientific Publications Team at Asan Medical Center for his editorial assistance in preparing this manuscript.

This research was supported by grants of the Korea Health Technology R&D Project through the Korea Health Industry Development Institute (funded by the Ministry of Health & Welfare, Republic of Korea, no. HI15C3078), Asan Institute for Life Sciences (no. 2014-585), and NIH CA152756 and CA150964 (S.D.M.).

References

[1] Siegel RL, Miller KD, and Jemal A (2016). Cancer statistics, 2016. *CA Cancer J Clin* **66**, 7–30.

[2] Lieberman DA (2009). Clinical practice. Screening for colorectal cancer. *N Engl J Med* **361**, 1179–1187.

[3] Winawer SJ, Zauber AG, Ho MN, O'Brien MJ, Gottlieb LS, Sternberg SS, Waye JD, Schapiro M, Bond JH, and Panish JF, et al (1993). Prevention of colorectal cancer by colonoscopic polypectomy. The National Polyp Study Workgroup. *N Engl J Med* **329**, 1977–1981.

[4] Zauber AG, Winawer SJ, O'Brien MJ, Lansdorp-Vogelaar I, van Ballegooijen M, Hankey BF, Shi W, Bond JH, Schapiro M, and Panish JF, et al (2012). Colonoscopic polypectomy and long-term prevention of colorectal-cancer deaths. *N Engl J Med* **366**, 687–696.

[5] Otto SL, Richard AK, and Jae Myung C (2014). Impact of sigmoidoscopy and colonoscopy on colorectal cancer incidence and mortality: an evidence-based review of published prospective and retrospective studies. *Intest Res* **12**, 268–274.

[6] Kahi CJ, Imperiale TF, Juliar BE, and Rex DK (2009). Effect of screening colonoscopy on colorectal cancer incidence and mortality. *Clin Gastroenterol Hepatol* **7**, 770–775 [quiz 711].

[7] Heresbach D, Barrioz T, Lapalus MG, Coumaros D, Bauret P, Potier P, Sautereau D, Boustiere C, Grimaud JC, and Barthelemy C, et al (2008). Miss rate for colorectal neoplastic polyps: a prospective multicenter study of back-to-back video colonoscopies. *Endoscopy* **40**, 284–290.

[8] Nam Hee K, Yoon Suk J, Woo Shin J, Hyo-Joon Y, Soo-Kyung P, Kyuyong C, and Dong II P (2017). Miss rate of colorectal neoplastic polyps and risk factors for missed polyps in consecutive colonoscopies. *Intest Res* **15**, 411–418.

[9] Chang Joon K, Yoon Suk J, Jung Ho P, Hong Joo K, Yong Kyun C, Chong Il S, Woo Kyu J, Byung Ik K, Shin Yeong L, and Hwa Mok K, et al (2013). Prevalence, clinicopathologic characteristics, and predictors of interval colorectal cancers in Korean population. *Intest Res* **11**, 178–183.

[10] Rutter M, Bernstein C, Matsumoto T, Kiesslich R, and Neurath M (2004). Endoscopic appearance of dysplasia in ulcerative colitis and the role of staining. *Endoscopy* **36**, 1109–1114.

[11] Itzkowitz SH and Harpaz N (2004). Diagnosis and management of dysplasia in patients with inflammatory bowel diseases. *Gastroenterology* **126**, 1634–1648.

[12] Wong Z, Shanthi P, and Raja Ali RA (2014). Inflammatory bowel disease-related colorectal cancer in the Asia-Pacific region: past, present, and future. *Intest Res* **12**, 194–204.

[13] Lutgens MW, Vleggaar FP, Schipper ME, Stokkers PC, van der Woude CJ, Hommes DW, de Jong DJ, Dijkstra G, van Bodegraven AA, and Oldenburg B, et al (2008). High frequency of early colorectal cancer in inflammatory bowel disease. *Gut* **57**, 1246–1251.

[14] Itzkowitz S (2003). Colon carcinogenesis in inflammatory bowel disease: applying molecular genetics to clinical practice. *J Clin Gastroenterol* **36**, S70–S74 [discussion S94-76].

[15] Yoon SM, Kim I-W, Song M, Do E-J, Ryu JH, Kim K, Kwon IC, Kim MJ, Moon DH, and Yang D-H, et al (2013). Near-infrared fluorescence imaging using a protease-activatable nanoprobe in tumor detection: comparison with narrow-band imaging. *Intest Res* **11**, 268–275.

[16] Kim SY and Myung SJ (2013). Optical molecular imaging for diagnosing intestinal diseases. *Clin Endosc* **46**, 620–626.

[17] Atreya R and Goetz M (2013). Molecular imaging in gastroenterology. *Nat Rev Gastroenterol Hepatol* **10**, 704–712.

[18] Joshi BP, Liu Z, Elahi SF, Appelman HD, and Wang TD (2012). Near-infrared–labeled peptide multimer functions as phage mimic for high affinity, specific targeting of colonic adenomas in vivo (with videos). *Gastrointest Endosc* **76**, 1197–1206.e1191-1195.

[19] Goetz M and Wang TD (2010). Molecular imaging in gastrointestinal endoscopy. *Gastroenterology* **138**, 828–833.e821.

[20] Kelly K, Alencar H, Funovics M, Mahmood U, and Weissleder R (2004). Detection of invasive colon cancer using a novel, targeted, library-derived fluorescent peptide. *Cancer Res* **64**, 6247–6251.

[21] Hsiung PL, Hardy J, Friedland S, Soetikno R, Du CB, Wu AP, Sahbaie P, Crawford JM, Lowe AW, and Contag CH, et al (2008). Detection of colonic dysplasia in vivo using a targeted heptapeptide and confocal microendoscopy. *Nat Med* **14**, 454–458.

[22] Goetz M, Ziebart A, Foersch S, Vieth M, Waldner MJ, Delaney P, Galle PR, Neurath MF, and Kiesslich R (2010). In vivo molecular imaging of colorectal cancer with confocal endomicroscopy by targeting epidermal growth factor receptor. *Gastroenterology* **138**, 435–446.

[23] Liu Z, Miller SJ, Joshi BP, and Wang TD (2013). In vivo targeting of colonic dysplasia on fluorescence endoscopy with near-infrared octapeptide. *Gut* **62**, 395–403.

[24] Hilderbrand SA and Weissleder R (2010). Near-infrared fluorescence: application to in vivo molecular imaging. *Curr Opin Chem Biol* **14**, 71–79.

[25] Kobayashi H, Ogawa M, Alford R, Choyke PL, and Urano Y (2010). New strategies for fluorescent probe design in medical diagnostic imaging. *Chem Rev* **110**, 2620–2640.

[26] Hawrysz DJ and Sevick-Muraca EM (2000). Developments toward diagnostic breast cancer imaging using near-infrared optical measurements and fluorescent contrast agents. *Neoplasia* **2**, 388–417.

[27] Ntziachristos V, Bremer C, and Weissleder R (2003). Fluorescence imaging with near-infrared light: new technological advances that enable in vivo molecular imaging. *Eur Radiol* **13**, 195–208.

[28] Mitsunaga M, Kosaka N, Choyke PL, Young MR, Dextras CR, Saud SM, Colburn NH, Sakabe M, Nagano T, and Asanuma D, et al (2013). Fluorescence endoscopic detection of murine colitis-associated colon cancer by topically applied enzymatically rapid-activatable probe. *Gut* **62**, 1179–1186.

[29] Park Y, Ryu YM, Jung Y, Wang T, Baek Y, Yoon Y, Bae SM, Park J, Hwang S, and Kim J, et al (2014). Spraying quantum dot conjugates in the colon of live animals enabled rapid and multiplex cancer diagnosis using endoscopy. *ACS Nano* **8**, 8896–8910.

[30] Xin B, Platzer P, Fink SP, Reese L, Nosrati A, Willson JK, Wilson K, and Markowitz S (2005). Colon cancer secreted protein-2 (CCSP-2), a novel candidate serological marker of colon neoplasia. *Oncogene* **24**, 724–731.

[31] Miller SJ, Joshi BP, Feng Y, Gaustad A, Fearon ER, and Wang TD (2011). In vivo fluorescence-based endoscopic detection of colon dysplasia in the mouse using a novel peptide probe. *PLoS One* **6**, e17384.

[32] Pierce MC, Javier DJ, and Richards-Kortum R (2008). Optical contrast agents and imaging systems for detection and diagnosis of cancer. *Int J Cancer* **123**, 1979–1990.

[33] Seaman ME, Contino G, Bardeesy N, and Kelly KA (2010). Molecular imaging agents: impact on diagnosis and therapeutics in oncology. *Expert Rev Mol Med* **12**, e20.

[34] Maeda H, Fang J, Inutsuka T, and Kitamoto Y (2003). Vascular permeability enhancement in solid tumor: various factors, mechanisms involved and its implications. *Int Immunopharmacol* **3**, 319–328.

[35] Ogawa M, Regino CA, Choyke PL, and Kobayashi H (2009). In vivo target-specific activatable near-infrared optical labeling of humanized monoclonal antibodies. *Mol Cancer Ther* **8**, 232–239.

[36] Maffione AM, Marzola MC, Capirci C, Colletti PM, and Rubello D (2015). Value of (18)F-FDG PET for predicting response to neoadjuvant therapy in rectal cancer: systematic review and meta-analysis. *AJR Am J Roentgenol* **204**, 1261–1268.

[37] Pita-Fernandez S, Alhayek-Ai M, Gonzalez-Martin C, Lopez-Calvino B, Seoane-Pillado T, and Pertega-Diaz S (2015). Intensive follow-up strategies improve outcomes in nonmetastatic colorectal cancer patients after curative surgery: a systematic review and meta-analysis. *Ann Oncol* **26**, 644–656.

[38] Lee S, Xie J, and Chen X (2010). Peptides and peptide hormones for molecular imaging and disease diagnosis. *Chem Rev* **110**, 3087–3111.

[39] Joshi BP, Dai Z, Gao Z, Lee JH, Ghimire N, Chen J, Prabhu A, Wamsteker EJ, Kwon RS, and Elta GH, et al (2016). Detection of sessile serrated adenomas in proximal colon using wide-field fluorescence. *Endosc Gastroenterol*.